FLAMMABILITY OF METHANE, PROPANE, AND HYDROGEN GASES

by Kenneth L. Cashdollar, Isaac A. Zlochower, Gregory M. Green, and Richard A. Thomas

Pittsburgh Research Laboratory
National Institute for Occupational Safety and Health
Pittsburgh, PA, U.S.A.

and Martin Hertzberg[1]

Copper Mountain, CO, U.S.A.

PROCEEDINGS OF THE

International Symposium on Hazards, Prevention, and Mitigation of Industrial Explosions

COLLOQUIUM ON GAS, VAPOR, HYBRID AND FUEL-AIR EXPLOSIONS

Schaumburg, Illinois, 21 – 25 September, 1998

FLAMMABILITY OF METHANE, PROPANE, AND HYDROGEN GASES

by Kenneth L. Cashdollar, Isaac A. Zlochower, Gregory M. Green, and Richard A. Thomas

Pittsburgh Research Laboratory
National Institute for Occupational Safety and Health
Pittsburgh, PA, U.S.A.

and Martin Hertzberg[1]

Copper Mountain, CO, U.S.A.

Abstract

This paper reports the results of Pittsburgh Research Laboratory flammability studies on methane, propane, hydrogen, and deuterium gases in air. Knowledge of the explosion hazards of these gases is important to the coal mining industry and to other industries that generate or use flammable gases. The experimental research was conducted in 20-L and 120-L closed explosion chambers under both quiescent and turbulent conditions, using both electric spark and pyrotechnic ignition sources. The data reported here generally confirm the data of previous investigators, but they are more comprehensive than those reported previously. The results illustrate the complications associated with buoyancy, turbulence, selective diffusion, and ignitor strength versus chamber size. Although the lower flammable limits (LFLs) are well defined for methane (CH_4) and propane (C_3H_8), the LFLs for hydrogen (H_2) and its heavier isotope deuterium (D_2) are much more dependent on the limit criterion chosen. A similar behavior is observed for the upper flammable limit of propane. The data presented include lower and upper flammable limits, maximum pressures, and maximum rates of pressure rise. The rates of pressure rise, even when "normalized" by the cube root of the chamber volume ($V^{1/3}$), are shown to be sensitive to chamber size.

[1]private consultant, retired from the U.S. Bureau of Mines

Introduction

Previous gas flammability limit data were obtained mainly in 5- to 10-cm-diameter flammability tubes, with lengths ten to thirty times the diameter, using spark ignition sources. Those flammability data are summarized in three Bureau of Mines bulletins (*1-3*). In those previous tests, a gas mixture in a vertical tube was ignited and flame propagation was determined by a visual criterion. To measure upward flame propagation, the gas mixture would be ignited at the bottom of the tube and the flame would travel upward to the top of the tube. To measure downward flame propagation, the gas mixture would be ignited at the top of the tube and the flame would travel downward.

The purpose of the present research was to obtain fundamental gas flammability data by measuring the pressure rise in closed chambers of different volumes. The gases studied were methane (CH_4), propane (C_3H_8), normal hydrogen (H_2), and its heavier isotope deuterium (D_2). The flammability data are essential for a quantitative risk assessment of the explosion hazard associated with the use of these gases. These gases are widely used (except D_2) and have widely varying molecular weights and diffusivities relative to oxygen. The effect of relative diffusivity of fuel and oxygen on the flammable behavior of mixtures near the flammability limits can influence those limits and the appropriate criteria for distinguishing between a flammable and nonflammable concentration (*4,5*). Methane, propane, and hydrogen are also used as standards with which other flammable gases can be compared. The gas flammability tests reported here were conducted at the Pittsburgh Research Laboratory[2] (PRL) in 20-L and 120-L chambers using standard test procedures developed by the PRL for similar studies. Some earlier data from a 25.5-m^3 sphere at PRL are also included. The flammability data reported include lean or lower flammable limits, rich or upper flammable limits, peak explosion pressures, and maximum rates of pressure rise. The tests were performed at ambient temperature and pressure under both quiescent and turbulent conditions. Some of the data in this report were presented previously in reference *6* and in two contract reports to DOE and its site contractors (*7,8*).

Test Chambers and Experimental Procedures

The flammability data for this report were obtained in 20-L, 120-L, and 25,500-L (25.5-m^3) chambers. The majority of the data are from the 120-L spherical chamber shown in figure 1. The internal diameter of the chamber is 60 cm, and its pressure rating is 69 bar. Instrumentation included a sensitive strain gauge pressure transducer to measure the partial pressures as the gases were added and mixed, two strain gauge pressure transducers to monitor the explosion pressure, and a silicon photodiode flame sensor. The strain gauges had a response time of ~ 1 ms. For some of the tests, a piezoelectric pressure transducer (with a response time of ~ 1 μs) was used. The pressure transducers were usually mounted on the top and bottom flanges of the chamber as shown in figure 1, but sometimes they were

[2]Many of these data were collected while the PRL was part of the U.S. Bureau of Mines, before its transfer to the National Institute for Occupational Safety and Health (NIOSH) in October 1996.

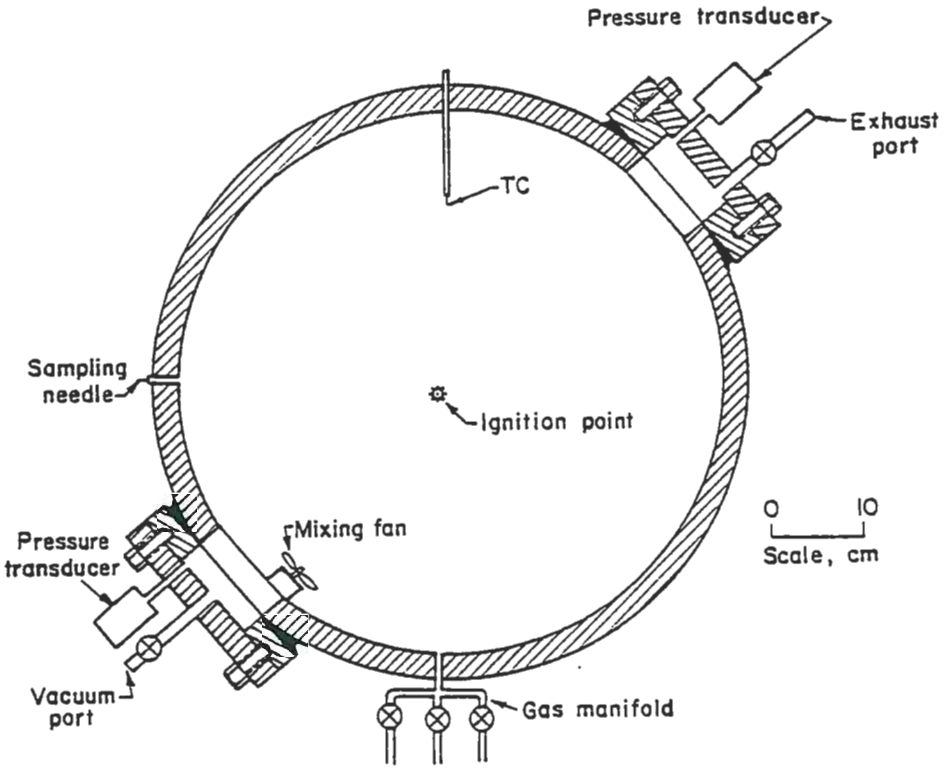

Figure 1. 120-L flammability test sphere.

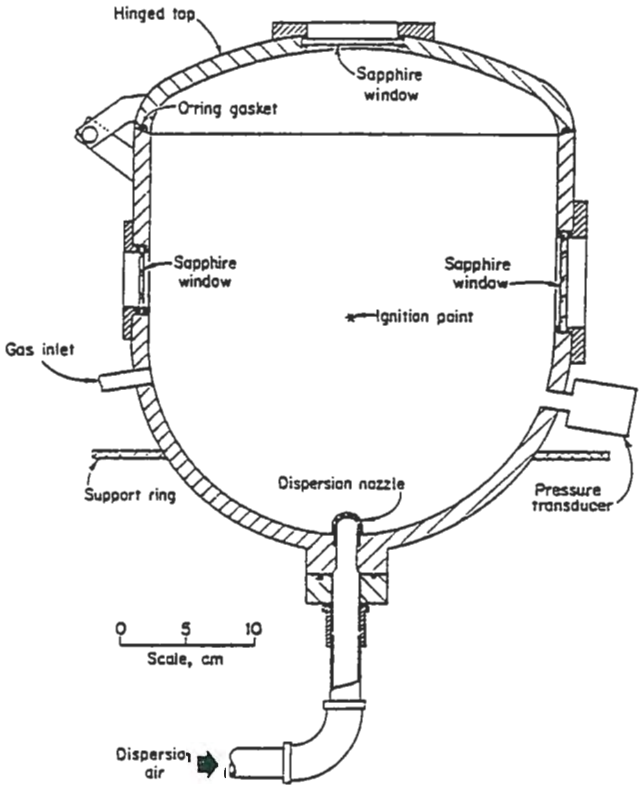

Figure 2. 20-L flammability test chamber

mounted on the sides of the chamber. For most of the tests, the flame sensor was mounted on the top flange to observe the flame radiation and, more importantly, to detect the spark radiation. This would confirm that the spark ignition source was working properly for tests in which the mixture did not ignite. For some of the tests, a fine wire thermocouple near the top of the chamber was used to record the gas flame temperature. The spark electrodes were located slightly below center. An internal fan was used to mix the gases.

Two "20-L" chambers (figure 2) were also used for the gas flammability tests. One had a volume of 19½ L and the other had a volume of about 21 L. For this report, both will be referred to as 20-L chambers. Each is a nearly spherical vessel made of 13-mm thick stainless steel (type 304) with a pressure rating of 21 bar. The approximate dimensions are 35 to 37 cm in height and 30 cm in diameter. Two strain gauges were used to measure the explosion pressure. The sapphire windows allowed visual observation of the tests. There were ports with ball valves for connection to a vacuum pump, vent, and a sensitive pressure transducer for gas addition by partial pressure. There were ports with needle valves for connection to sources of compressed dry air and the fuel gases. There was a solenoid controlled port on the bottom for the rapid introduction of compressed air to assist in mixing the gases. In other tests, a fan was used to mix the gases. The spark electrodes were located slightly below center.

The calibrations of the pressure transducers for both the 20-L and 120-L chambers were checked daily using the internal shunt calibration resistors provided by the manufacturers. At the start of a test, the chamber was evacuated, and then the various gases were added at the partial pressures required to give the desired mixture composition. A non-sparking internal fan was used for mixing the gases in the 120-L chamber and for some of the tests in the 20-L chambers. When the fan was used, the gases were mixed for at least 3 to 4 min before each test, and the fan was turned off 1 min prior to ignition to provide a well mixed, quiescent system. The absolute pressure at ignition was about 1 bar or 1 atm. Samples of the gas mixtures could be collected in evacuated test tubes through a sampling needle on the side of the chamber. These samples would then be analyzed by gas chromatography (GC). During the initial evaluation of the mixing efficiency in the 120-L chamber, samples of H_2-air mixtures were collected at t = 0 min (after all of the gases had been added to the chamber) and after 2 and 5 min of mixing by the fan. There was essentially no difference in the measured concentrations of H_2 for the gas mixtures over this time period, showing that there was good mixing of the gases even before the fan was turned on. For some of the H_2 tests in the 20-L chamber, the fuel gas was added first and then the air was added rapidly through the solenoid valve as a way of mixing the gases. The data showed no difference from the fan mixed case. The reported fuel concentrations are in mole (volume) percent, based on the fuel and total pressures.

Both the 20-L and 120-L chambers had similar spark ignition systems. The electrodes were 3 mm diameter brass rods. In some cases, the brass rods were sharpened to a point. In other cases, steel phonographic needles were soldered to the ends of the rods. The electrodes were positioned slightly below center in the chambers, with a spark gap of

6 mm. For the 20-L tests, a 380 or 900 μf capacitor was charged to 300 V and then discharged at ignition through a transformer to generate a strong spark with a stored energy ($\frac{1}{2}CE^2$, where C is the capacitance and E is the voltage) of 17 or 40 J. The actual electrical energy in the spark gap may be considerably less because of the low efficiency of the transformer circuit (*9*). In the 20-L chamber, the measured pressure pulse due to the rapid heating (by the spark) of the air volume in the immediate vicinity of the electrode gap was ~4 mpsi. The corresponding delivered thermal energy ($2.5V\Delta P$, where V is the chamber volume and ΔP is the pressure rise) was about 1 J. For the 120-L tests, the standard ignition source was a strong electric spark from a 1300 μF capacitor at 300 V. This corresponded to a stored energy on the capacitor of $\frac{1}{2}CE^2 = 58$ J. The thermal energy of this spark was about 2 J, based on the measured pressure rise in a known volume. For practical comparisons, Lüttgens and Glor (*10*) and Eckhoff (*11*) report typical electrostatic spark energies in industrial practice of 15 mJ for a person to several hundred millijoules for major plant items such as large containers.

Much stronger, electrically-activated, pyrotechnic ignitors with calorimetric energies of 1,000 to 5,000 J were used for some of the tests in the 120-L chamber. These ignitors produce a large flame of hot particles; they are manufactured by Fr. Sobbe[3] of Germany and distributed by Cesana Corp. of Verona, NY. The energy of the 5,000-J ignitor is somewhat higher than that of two books of pocket matches, all ignited at once.

For a test with initially "turbulent" conditions in the 120-L chamber, the mixing fan was left on during the test. The fan was located near the bottom flange as shown in figure 1, and the gas flow was directed toward the ignition point. The fan had an 8-cm diameter blade that rotated at 3000 rpm. The flow characteristics of the fan were measured in open air outside the chamber. The air flow velocity along the axis of rotation was ~1.4 m/s at 15 cm, ~1.1 m/s at 30 cm, and ~0.7 to ~1.1 m/s at 45 cm from the fan blade. The turbulence level generated by the fan was not directly measured; the fan was used only to determine whether moderate turbulence had a significant effect on the flammability data of the various gases near the lower flammable limit.

The data from the pressure transducers, the flame sensor, and the thermocouple were recorded using a high speed analog-to-digital (A/D) board in a personal computer (PC). This system can sample the data from various instrument channels, usually at speeds less than 20 kHz per channel. A PRL designed computer software program converted the raw data to engineering units, plotted the data versus time, and allowed various data smoothing options. Maximum pressure and maximum rate of pressure rise values were obtained from the pressure versus time traces. Data from the two pressure transducers were compared and averaged if they agreed to within 5%. If they did not agree to within 5%, the two pressure transducers were checked to determine the reason for the difference. The reproducibility of the flammability data was checked by repeat tests over a period of months or years.

---

[3]Mention of any company name or product does not constitute endorsement by NIOSH.

Some earlier PRL data by other authors (*12-15*) in a much larger 25.5-m^3 chamber are included for comparison purposes. This spherical chamber had an internal diameter of 3.65 m and a pressure rating of 21 bar.

Thermodynamic Calculations

Adiabatic equilibrium calculations of product gas temperatures, pressures, and compositions were made for the various fuel gas and air mixtures. The calculations give the maximum expected explosion temperatures and pressures for the gas mixtures in the absence of a detonation. A comparison of the experimentally measured pressures with the calculated adiabatic pressures would indicate the degree of adiabaticity of the explosion and the extent of reaction of the fuel-air mixture.

The calculations were generated on Digital Electronic Corp. VAX computers using the CEC-80 Fortran code for the computation of complex equilibrium calculations that was developed at the NASA-Lewis Research Center (*16*). This program computes the equilibrium product composition from the listed reactants and their standard energies of formation by examining all possible product species (consisting of combinations of the reactant atoms) whose temperature dependent thermodynamic properties are listed in an auxiliary table. The thermodynamic properties accessed by the program are taken predominantly from the JANAF thermodynamic data compilation (*17*). The product composition is obtained by minimizing the free energy of the system. Constant volume calculations were used to compare the experimentally measured pressures to the adiabatic equilibrium pressures. Constant pressure calculations were also performed at one atmosphere to determine the adiabatic temperatures. Such temperature calculations have been found useful in deriving limiting flame temperatures and compositions.

Experimental Data

Pressure Traces for Methane and Hydrogen

Figure 3 shows the pressure rise versus time traces for various gaseous mixtures of CH_4 and air, tested in the 120-L chamber. The mixtures were initially quiescent and a spark ignition source was used. Figure 3*A* shows data for a mixture of 5% CH_4 and 95% air. The pressure-time trace shows only a small pressure rise ($\sim$0.06 bar) and is typical of a mixture on the edge of flammability. There may be some burning near the spark but only limited upward propagation beyond the ignition source. The data in figure 3*B* are for 5.5% CH_4 and 94.5% air. For this test, there is a $\sim$0.7-bar pressure rise associated with upward and horizontal flame propagation. Upward propagation is easier than other propagation directions because combustion products are hotter and less dense than the reactants from which they are generated. The upward acceleration of the burned gas flame kernel aids upward flame propagation (*18,19*). Hence, upward propagation is always easier in the sense that leaner mixtures that can propagate upward may not be able to propagate downward. That is the case for the 5.5% CH_4 mixture in figure 3*B*. The data in figure 3*C* are for 6% CH_4 and

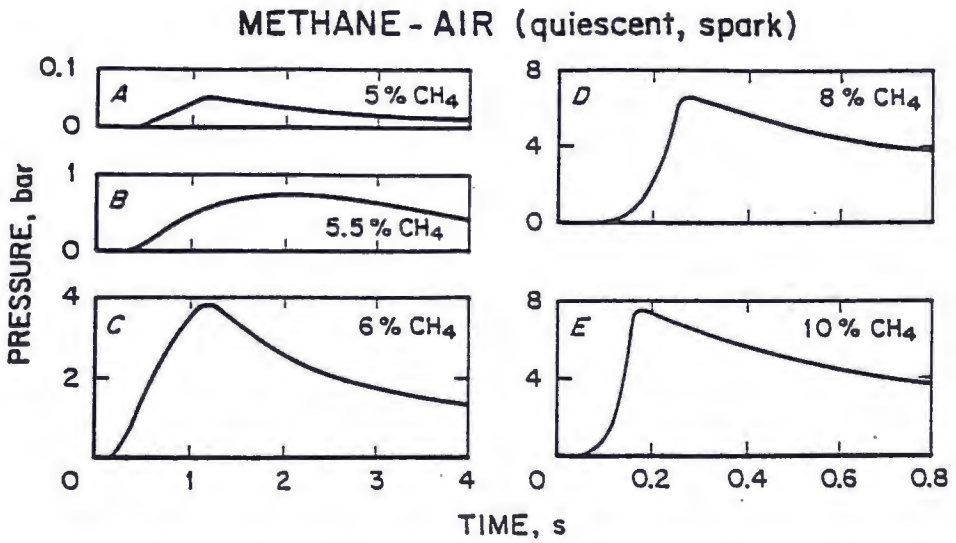

Figure 3. Pressure-time traces for mixtures of (*A*) 5% CH_4 in air, (*B*) 5.5% CH_4 in air, (*C*) 6% CH_4 in air, (*D*) 8% CH_4 in air, and (*E*) 10% CH_4 in air.

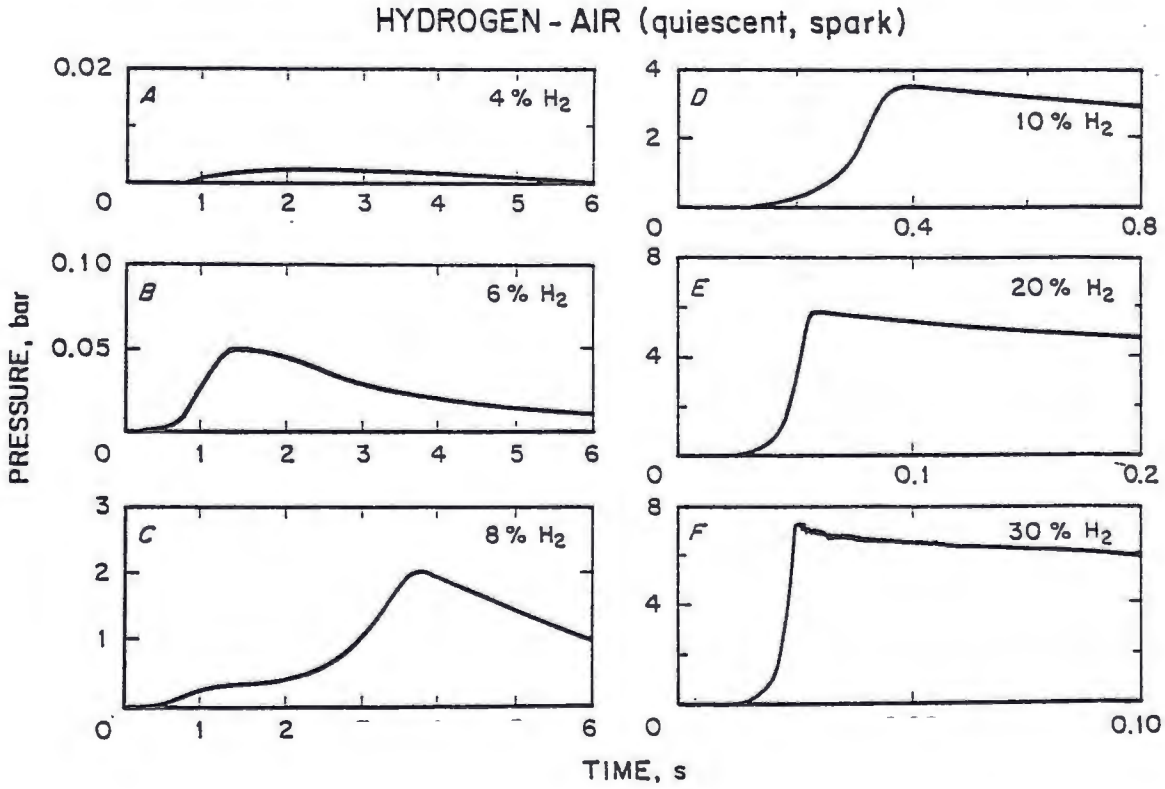

Figure 4. Pressure-time traces for mixtures of (*A*) 4% H_2 in air, (*B*) 6% H2 in air, (*C*) 8% H_2 in air, (*D*) 10% H_2 in air, (*E*) 20% H2 in air, and (*F*) 30% H2 in air.

94% air. For this test, there is a pressure rise of almost 4 bar, and there is significant flame propagation in the horizontal and downward directions in addition to upward. At 6% CH_4, the calculated pressure rise for adiabatic combustion is about 5.9 bar. Therefore, the flame had to propagate through more than half of the chamber in this case.

The data in figure 3*D* are for 8% CH_4 and 92% air. For this test, the propagation is rather rapid and nearly spherical. The measured peak explosion overpressure (~6½ bar) is close to the calculated, adiabatic equilibrium pressure (7.2 bar) for constant volume combustion, and most of the mixture is consumed. The data in figure 3*E* are for 10% CH_4 and 90% air. For this near-stoichiometric mixture, the flame speed is fast, and it takes less than 0.2 s for the flame to propagate from its point of ignition to the chamber wall (a distance of 30 cm). The measured peak explosion overpressure (~7½ bar) is close to the calculated, adiabatic equilibrium pressure (7.9 bar) for constant volume combustion, showing that the entire mixture is almost completely consumed.

Figure 4 shows the pressure rise versus time traces for various quiescent mixtures of H_2-air, tested in the 120-L chamber using a spark ignition source. Figure 4*A* shows data for a mixture of 4% H_2 and 96% air. The pressure-time trace shows only a very small pressure rise (~0.002 bar). This would not be considered propagation for most pressure rise criteria. The data in figure 4*B* are for 6% H_2 and 94% air. There is a small but measurable pressure rise (~0.05 bar) associated with propagation in the upward direction only. Hydrogen is an unusual fuel with both high reactivity and high diffusivity. The actual concentration at the surface of the highly curved and discrete flame kernels is appreciably higher than the overall concentration (*4,5*). At low H_2 concentrations, these highly buoyant, ascending flame kernels can propagate for significant distances while barely affecting the overall gas temperature, pressure, and composition (*1*).

The data in figure 4*C* are for a mixture containing 8% H_2 and 92% air, and the propagation is a two stage process. The early stage of the pressure-time trace is associated with upward and horizontal flame propagation. A hiatus occurs from 1 to 2 s at a pressure of ~0.3 bar as the upward propagating flame front reaches the top of the spherical chamber. The later, more rapid downward flame propagation results in the peak pressure of 2.0 bar at a time of 3 to 4 s. This shows that there is a transition to downward flame propagation at ~8% H_2.

The data in figure 4*D* are for a mixture containing 10% H_2 and 90% air. For this composition, the propagation dynamics are simpler and essentially isotropic. The propagation is rapid and nearly spherical, and this is reflected in a monotonic increase in pressure with time. Combustion is essentially complete before 0.4 s. The measured peak explosion overpressure (3.2 bar) is essentially the same as the calculated, adiabatic equilibrium pressure for constant volume combustion. The entire mixture is almost completely consumed as the spherical fireball reaches the wall almost simultaneously for all three directions of flame propagation (upward, downward, and horizontal). The pressure time trace in figure 4*E* is for a mixture containing 20% H_2 and 80% air. For this mixture,

the flame speed is very fast, it now takes only slightly less than 0.06 s for the flame to propagate from its point of ignition to the chamber wall (a distance of 30 cm). The measured peak explosion overpressure (5.6 bar) is essentially the same as the calculated, adiabatic equilibrium pressure. The pressure time trace in figure 4*F* is for a mixture containing 30% H_2 and 70% air. Here the flame speed is even faster and the high frequency pressure fluctuations (acoustic ringing) may be the start of a transition to a detonation. Again, the measured explosion pressure is essentially the same as the calculated adiabatic pressure.

Methane-air, quiescent, spark

A graphical summary of the data for mixtures of methane (CH_4) and air tested in the 20-L and 120-L chambers using spark ignition is shown in figure 5. At the bottom of the figure, the pressure ratio, PR, is the maximum absolute explosion pressure for each test divided by the initial absolute pressure:

$$PR = P_{max}/P_{initial} \tag{1}$$

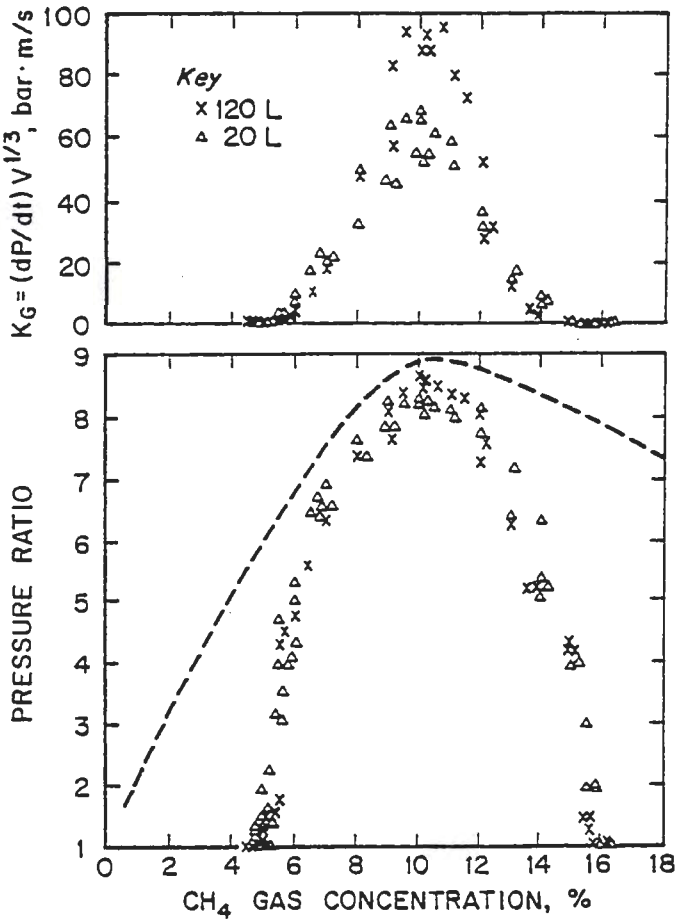

Figure 5. Flammability data for quiescent mixtures of methane (CH_4) in air in 20-L and 120-L chambers, compared to dashed curve for calculated adiabatic values.

Since the initial pressure for a test is approximately one bar or one atmosphere, the pressure ratio is approximately the absolute explosion pressure in bars or atmospheres. Subtracting the number 1 from the pressure ratio value would give the explosion pressure rise in bars or atmospheres. Taking the ratio of explosion pressure to initial pressure is a way of normalizing the data and correcting for slight variations in the starting test pressure. At the top of the figure, K_G is the maximum rate of pressure rise, $(dP/dt)_{max}$, for each test, normalized by the cube root of the chamber volume, V:

$$K_G = (dP/dt)_{max} V^{1/3} \qquad (2)$$

These CH_4 data in figure 5 are typical of those for hydrocarbon gases. There is a sharp discontinuity at the lower flammable limit near 5% and at the upper flammable limit near 16%. The explosion pressures and rates of pressure rise are highest at a concentration (~10%) that is slightly above the stoichiometric value of 9.5%. The pressure data for spark ignition in the two chambers are very similar, and the peak explosion pressures at ~10% CH_4 are close to the calculated, adiabatic equilibrium values (dashed curve). The 120-L peak pressures are slightly higher than those from the 20-L chamber, showing that the 120-L chamber explosions are more adiabatic. The normalized rates of pressure rise (K_G) in the two chambers are similar near the flammability limits, but the K_G-data from the larger chamber are higher near stoichiometric CH_4 concentrations. The most likely reason is that near-stoichiometric flame propagation in the larger, spherical chamber more nearly approximates ideal, adiabatic combustion.

The lean flammability limit region of figure 5 is shown in more detail in the expanded scale of figure 6. This graph also shows earlier data (*15*) from a 25.5-m^3 chamber at PRL. A reasonable criterion used previously (*20*) for upward flame propagation in air (using a spark ignition source in a closed vessel) is a pressure rise of at least 0.07 bar (1 psi) or at least 7% higher than the initial pressure of 1 bar. This corresponds to PR $\geq$ 1.07. Based on this propagation criterion, the lean flammable limit for upward flame propagation of methane in air in the 120-L chamber is LFL = 5.0±0.1%, using spark ignition. In the much larger 25.5-m^3 chamber, the LFL is 5.1±0.1% using the same pressure rise criterion. However, Burgess et al. (*15*) reported visual observations of upward flame travel at methane concentrations as low as 4.9% in the 25.5-m^3 chamber. The LFL values with either a pressure rise or visual criterion are consistent with the 5.0% LFL reported for upward propagation of methane-air flames in flammability tubes (*3*).

Methane-air, turbulent, spark

The data shown in figure 7 are for "turbulent" combustion of CH_4-air mixtures in the 120-L chamber. The initial turbulence level was induced by allowing the mixing fan to run continuously during the 120-L test. The purpose of these tests was to determine the effects of a moderate initial gas flow or turbulence on the flammability data at low CH_4 concentrations. These "turbulent" data (open circles) are compared with the data (solid curve) for the quiescent CH_4-air mixtures from figure 6. The calculated adiabatic explosion

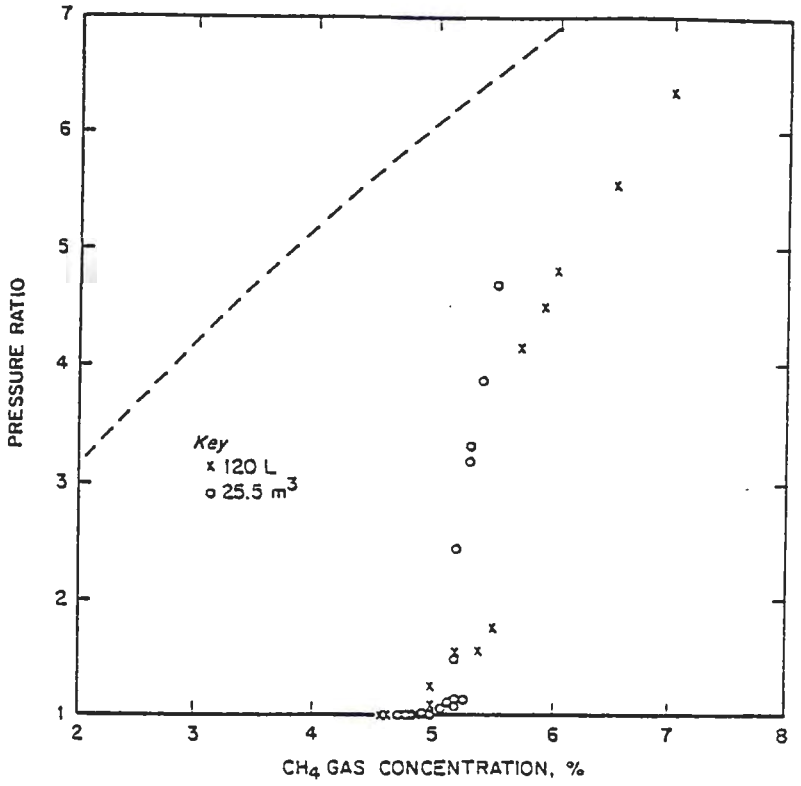

Figure 6. Lean limit flammability data for quiescent mixtures of methane in air in 120-L chamber, compared to earlier data from 25.5-m^3 chamber (Ref. *15*) and to dashed curve for calculated adiabatic values.

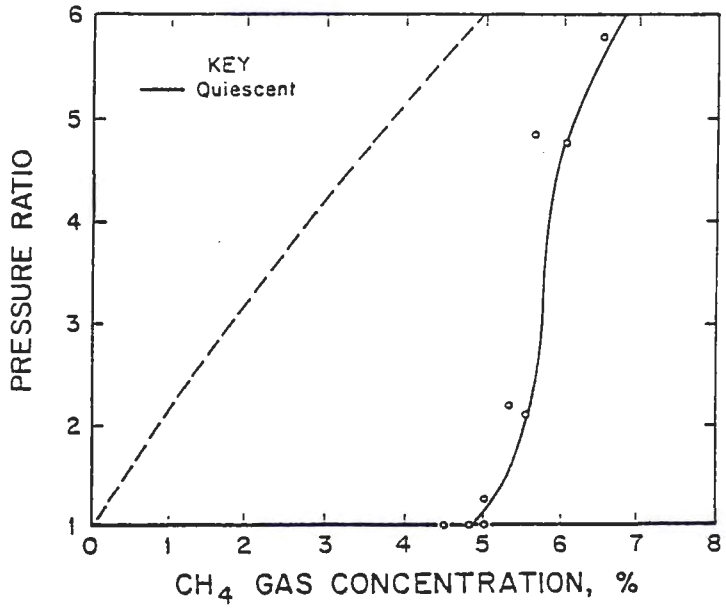

Figure 7. Lean limit flammability data (open circles) for "turbulent" mixtures of CH_4 in air in 120-L chamber, compared to solid curve for quiescent experimental data and to dashed curve for calculated adiabatic values.

pressure is again shown as the dashed curve. The measured pressure ratio data indicate that there is no significant difference between the "turbulent" and quiescent cases for CH_4-air near the lean limit.

Methane-air, quiescent, pyrotechnic ignitors

Figure 8 shows CH_4-air data for 1,000- and 5,000-J ignitors in the 120-L chamber. The experimental pressure data are again compared to the quiescent spark data (solid curve) and to the calculated, adiabatic equilibrium pressures (dashed curve). The pressure rise from the ignitor by itself was subtracted from the measured pressure for the data in the figure.

$$PR = (P_{max} - \Delta P_{ignitor})/P_{initial} \quad (3)$$

For the 1,000-J ignitors, this pressure was 0.025 bar and for the 5,000-J ignitors, it was 0.09 bar. The apparent lean limits using the Sobbe ignitors are somewhat lower than that measured with the electric spark source. However, the stronger Sobbe pyrotechnic ignitors have a much larger ignition volume than the spark, and all of the CH_4 in this volume would be combusted even without any propagation beyond the ignition volume. Therefore, it is reasonable to use a more stringent pressure rise criterion for flame propagation with the Sobbe ignitors. For this study, a criterion of PR $\geq$ 1.5 for upward propagation was chosen. (In previous studies using the 20-L chamber (*6*), a criterion of PR $\geq$ 2 was used for the

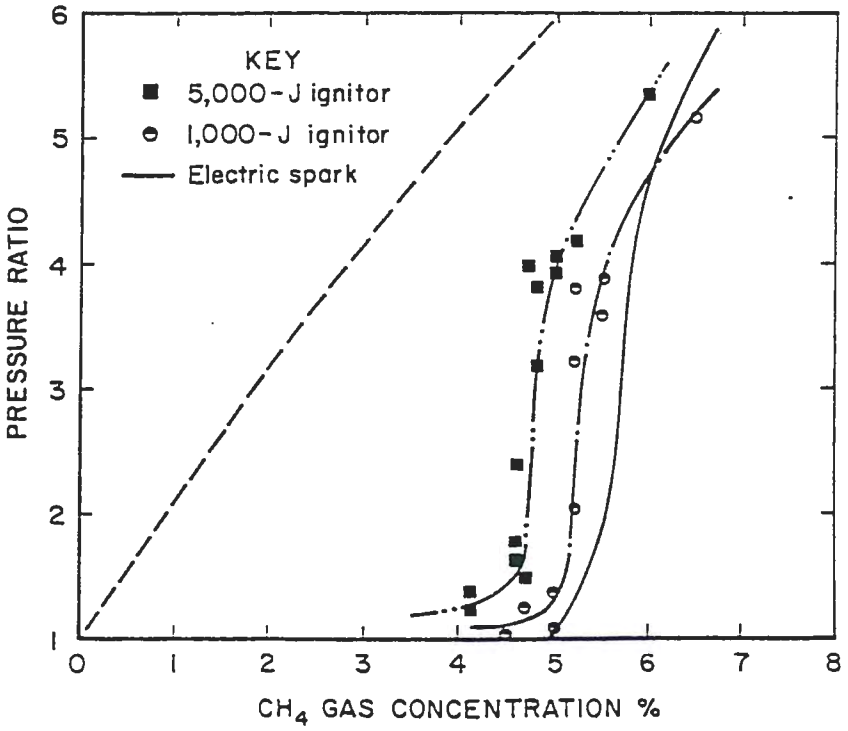

Figure 8. Flammability data for quiescent mixtures of CH_4 in air in 120-L chamber, using 1,000- or 5,000-J pyrotechnic ignitors, compared to solid curve for spark data and to dashed curve for calculated adiabatic values.

Sobbe ignitors since the ignitor volume represents a larger fraction of the 20-L chamber volume than for the 120-L chamber.) Using this PR $\geq$ 1.5 criterion, the methane-air limits in the 120-L chamber are: LFL = 4.6% for the 5000-J ignitor and LFL = 5.1% for the 1000-J ignitor. The lower LFL with the 5000-J ignitor indicates that this high energy pyrotechnic is "overdriving" the mixture somewhat in the 120-L chamber. The final conclusion for the methane-air data is that there is no major difference in the measured lean limit results with the different strength ignitors or for upward versus downward propagation.

Propane-air, quiescent, spark

The data for initially quiescent mixtures of propane (C_3H_8) in air shown in figure 9 are similar in form to the methane-air data in figure 5. There is a sharp discontinuity at the lower flammable limit near 2%. There is a fairly distinct drop in pressure near 8% C_3H_8, but there is also a tail of measurable pressures out to higher C_3H_8 concentrations. Based on a pressure rise criterion of 7%, the LFL of propane is 2.05 ± 0.05% and the UFL is -9.8 ± 0.2%. These limits correspond to upward flame propagation that consumes only a small fraction of the flammable gas mixture. The LFL for downward propagation would be slightly above 2% since the discontinuity is very sharp at the LFL. However, the UFL for downward propagation would be 7½% to 8% C_3H_8, significantly lower than the UFL for upward propagation. This is probably due to the greater diffusivity of oxygen (0.43 cm^2/s) relative that of propane (0.25 cm^2/s) (5). The oxygen can selectively diffuse into the flame front, enriching it in oxygen. This effect could allow rich mixtures that would not normally be flammable to propagate upward in a narrow cone angle.

In figure 9, the propane explosion pressures and rates of pressure rise are highest at a concentration ($-4\frac{1}{2}$% to 5%) that is slightly above the stoichiometric value of 4.0%. The maximum explosion pressures are close to the calculated adiabatic values. The maximum explosion pressures for the propane are somewhat higher than those for methane, in accord with its higher reactivity. The maximum K_G values for the propane-air mixtures are considerably higher than those for methane-air.

Hydrogen-air, quiescent, spark

The data for initially quiescent hydrogen-air mixtures with spark ignition in the 120-L chamber are shown in figure 10. The measured peak explosion pressure ratios and the size normalized rates of pressure rise are plotted as a function of hydrogen concentration in air. The measured pressure ratios are compared with the calculated, adiabatic equilibrium explosion pressures for constant volume combustion (dashed curve). For hydrogen concentrations above 10% where the propagation is rapid and isotropic and the complications associated with buoyancy are minimal, there is good agreement between the measured pressure ratios and those calculated for adiabatic equilibrium. The maximum explosion pressures and rates of pressure rise are found at a H_2-concentration that is slightly above the stoichiometric value of 29.5%.

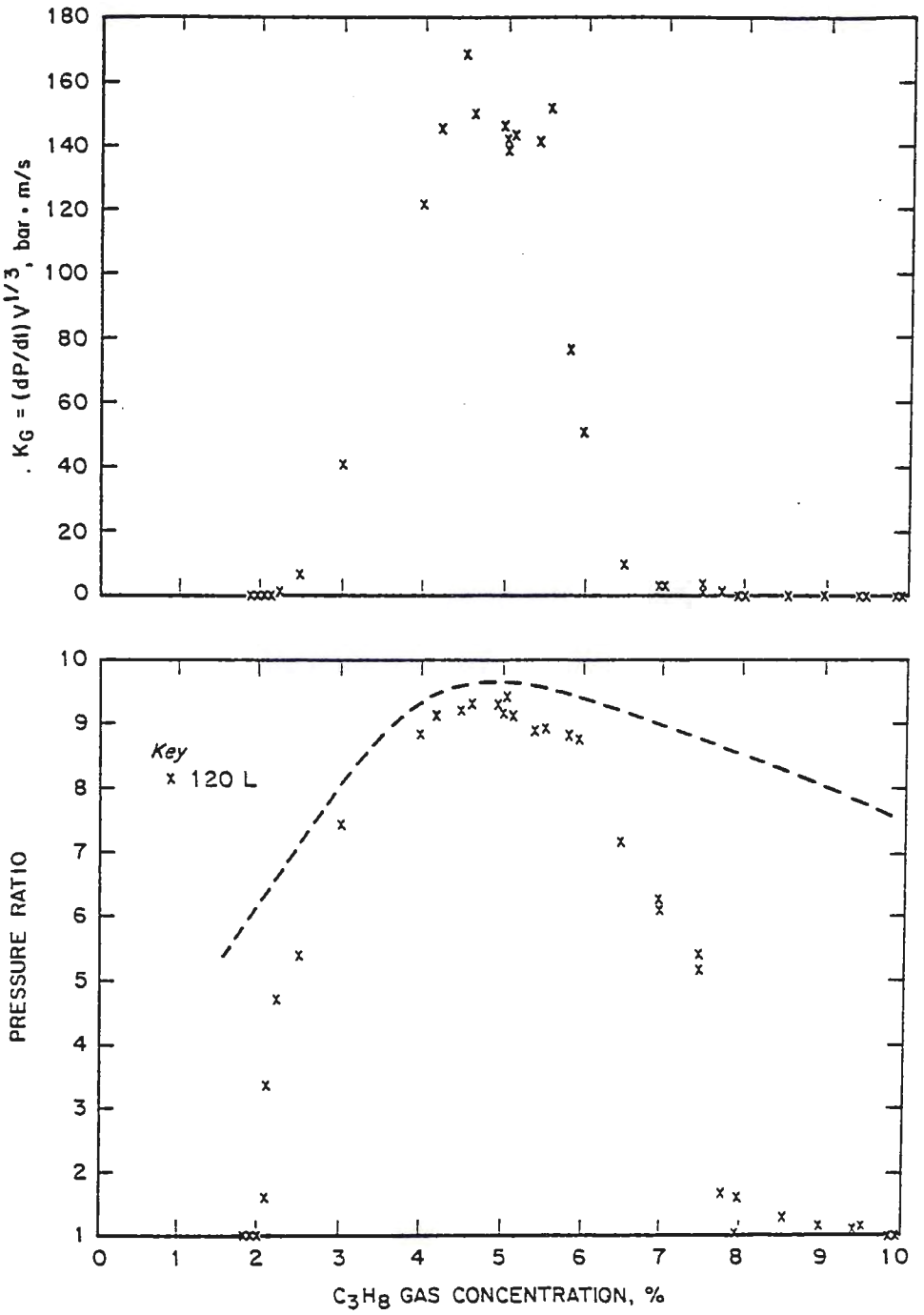

Figure 9. Flammability data for quiescent mixtures of propane (C_3H_8) in air in 120-L chamber, compared to dashed curve for calculated adiabatic values.

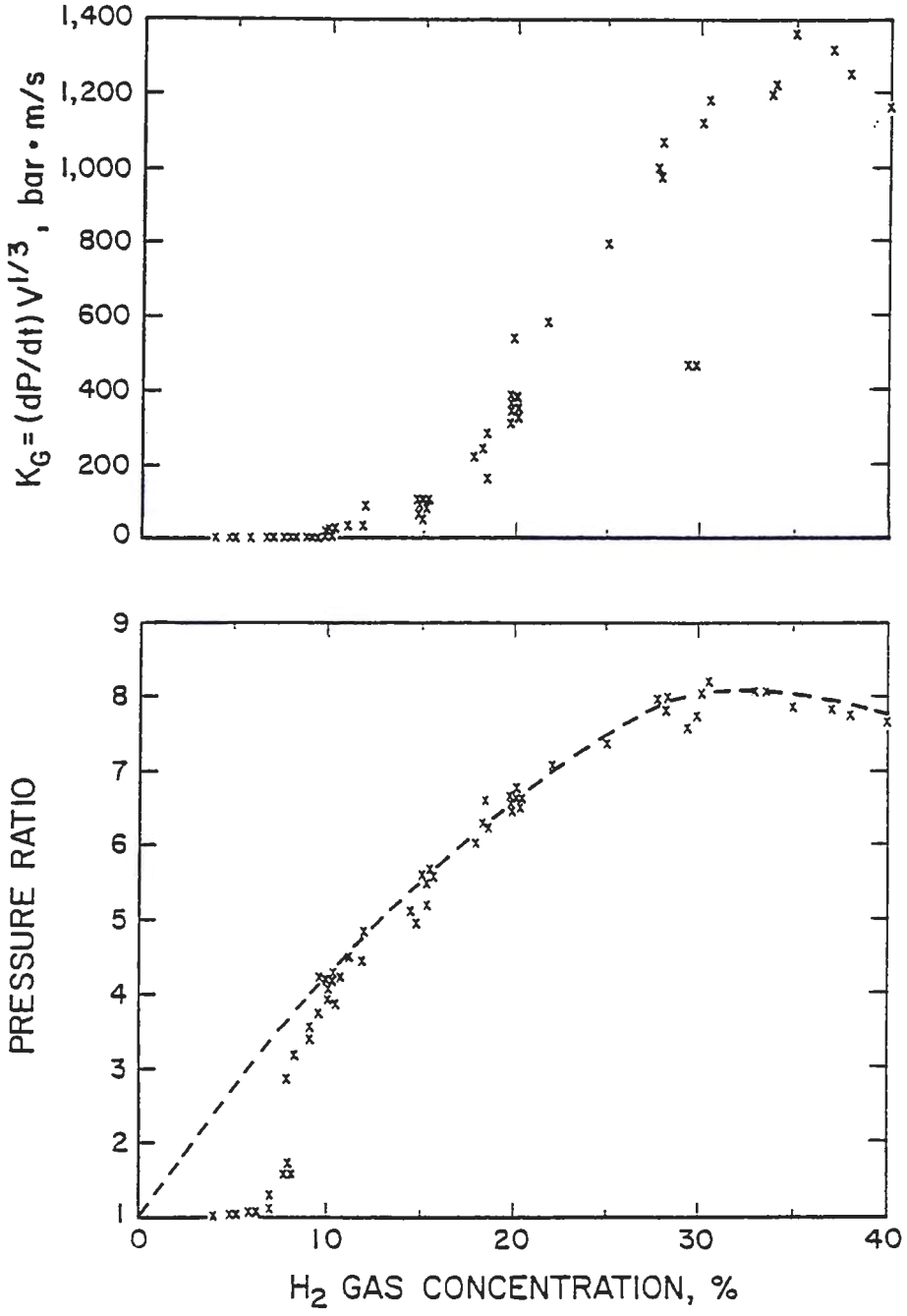

Figure 10. Flammability data for quiescent mixtures of hydrogen (H_2) in air in 120-L chamber, compared to dashed curve for calculated adiabatic values.

The lower concentration H_2-data are shown in an expanded scale in figure 11. The pressures are very low at concentrations less than 8% H_2. The complexities associated with low H_2 concentrations have already been discussed in relation to the pressure time traces shown in figure 4. The data for the H_2-air mixtures shown in figure 11 display essentially the same combination of two stage flame propagation at ~8% H_2. There is a rapid increase in the measured pressure ratio at ~8% H_2, and that near-discontinuity corresponds to the lean limit for downward flame propagation. In the earlier PRL hydrogen tests in the 25.5-m^3 sphere (*12*), the limit for downward flame propagation was slightly higher, 8½% H_2. As indicated earlier, in the presence of buoyancy, complete consumption of the unburned mixture is possible in the sphere only if the downward propagation occurs. Once that downward lean limit is exceeded (H_2 > 8%), complete combustion is possible, and the measured explosion pressures approach the calculated adiabatic values at ~10% H_2.

Hydrogen flammability data from the 20-L and 120-L chambers over the 3% to 9% H_2 region are shown on a greatly expanded scale in figure 12. For concentrations less

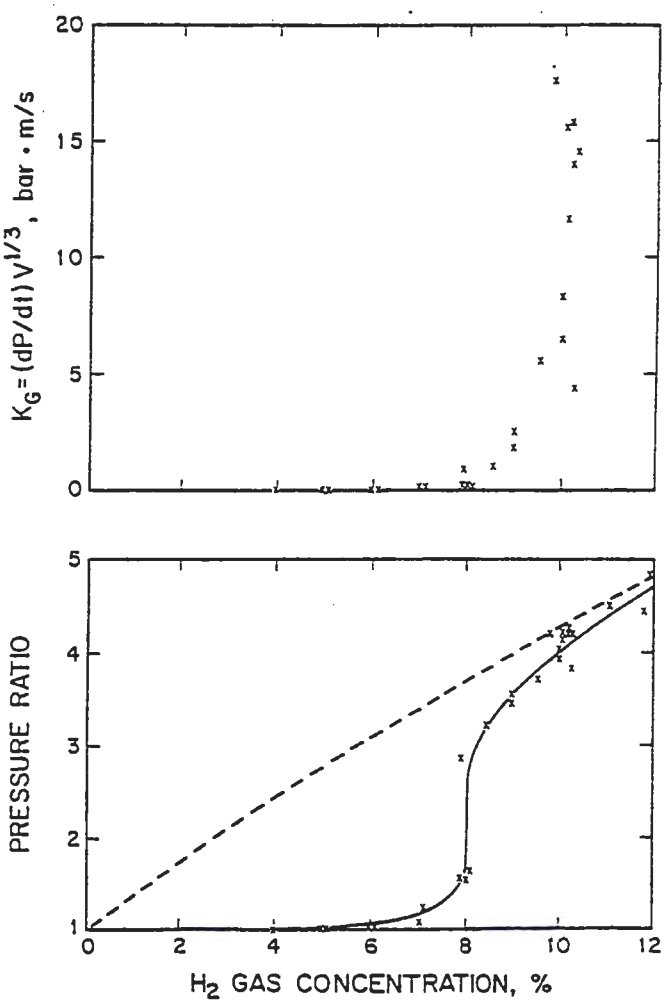

Figure 11. Expanded scale flammability data for quiescent mixtures of hydrogen in air in 120-L chamber, compared to dashed curve for calculated adiabatic values.

than the downward limit of ~8% H_2, only upward propagation is possible in the quiescent mixture. This upward propagation occurs in a narrow cone angle above the spark. For concentrations <8% H_2, the volume of the unburned mixture consumed in that cone angle is so much smaller than the total spherical test volume that measured explosion pressures are only a small fraction of the calculated adiabatic values for complete combustion. An explanation for this phenomenon is that fresh hydrogen selectively diffuses into the flame front more rapidly than oxygen does, thus enriching the flame in hydrogen (*1,4,5,21*). The diffusivity of hydrogen is 1.86 cm^2/s, much larger than the 0.43-cm^2/s value for oxygen (*5*). Based on the previous criterion of a 7% pressure rise or PR ≥ 1.07, the LFL ≈ 6±½% for H_2-air in the 20-L chamber and LFL ≈ 6½±½% for H_2-air in the 120-L chamber, using a spark ignition source. Based on a weaker criterion of a 3% pressure rise used in some previous studies (*8*), the LFL ≈ 5±½% for H_2-air in both the 20-L and 120-L chambers. These values are still higher than the LFL of 4% H_2 reported from flammability tubes (*3,22*), using a visual criterion for upward flame propagation. In figure 12, 4% H_2 corresponds to a point where the pressure versus H_2 concentration data curve reaches the x-axis at PR = 1.0 or at a pressure rise of 0.0 bar.

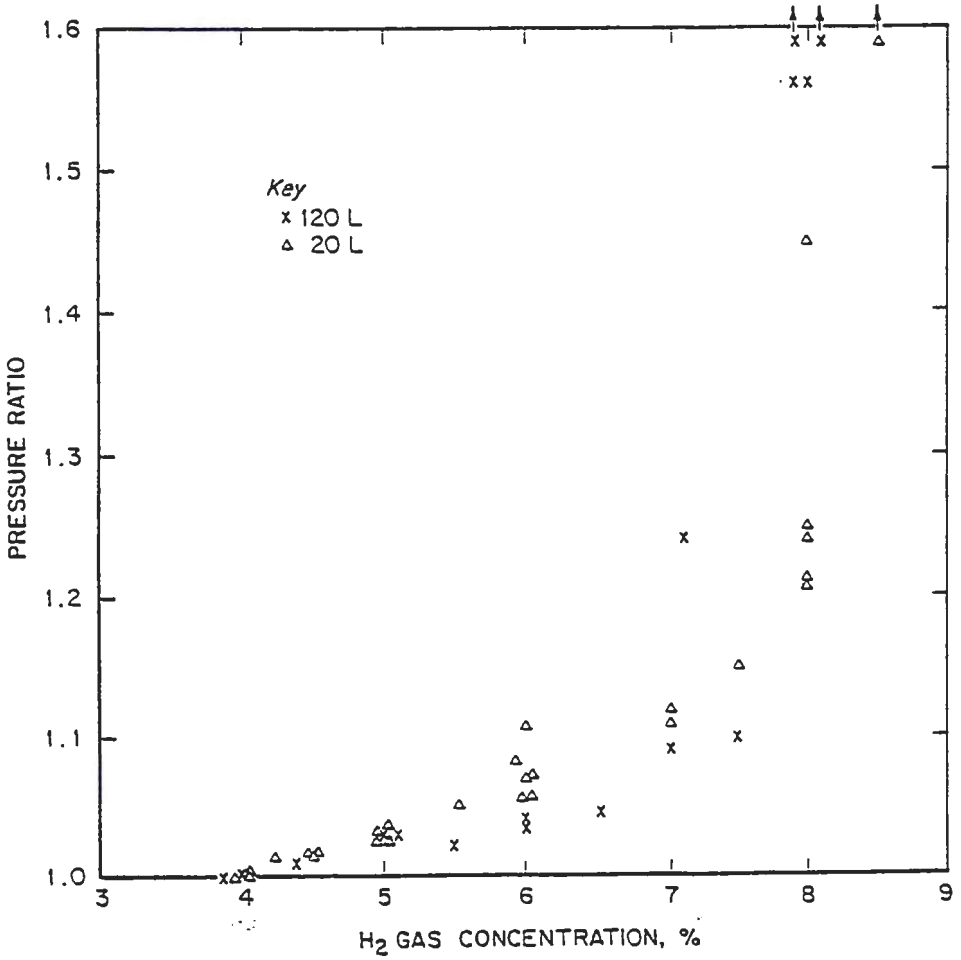

Figure 12. Lean limit flammability data for quiescent mixtures of hydrogen in air in 20-L and 120-L chambers.

Hydrogen-air, turbulent, spark

The data shown in figure 13 are for "turbulent" combustion of H_2-air mixtures. The initial turbulence level was induced by allowing the mixing fan to run continuously during the 120-L test. The purpose of these tests was to show the effects of moderate initial gas flow or turbulence on the flammability data at low H_2-concentrations. These "turbulent" data (open circles) are compared with the solid curve data for the quiescent H_2-air mixtures from figure 11. The calculated adiabatic explosion pressure is again shown as a dashed curve. The measured pressure ratio data points indicate that there is no significant difference between the "turbulent" and quiescent cases for H_2 concentrations above 10%, where the measured values under both initial conditions are close to the calculated adiabatic equilibrium explosion pressures. At the lower H_2-concentrations, however, there is no longer the sharp discontinuity associated with the downward limit near 8% H_2 that was observed for the quiescent (or laminar) case. Instead, for the "turbulent" case, there is an almost linear increase in the explosion pressure between 4% and 10% H_2. At 6% H_2, the measured pressure rise for the "turbulent" case is over one-half the calculated, adiabatic value. For

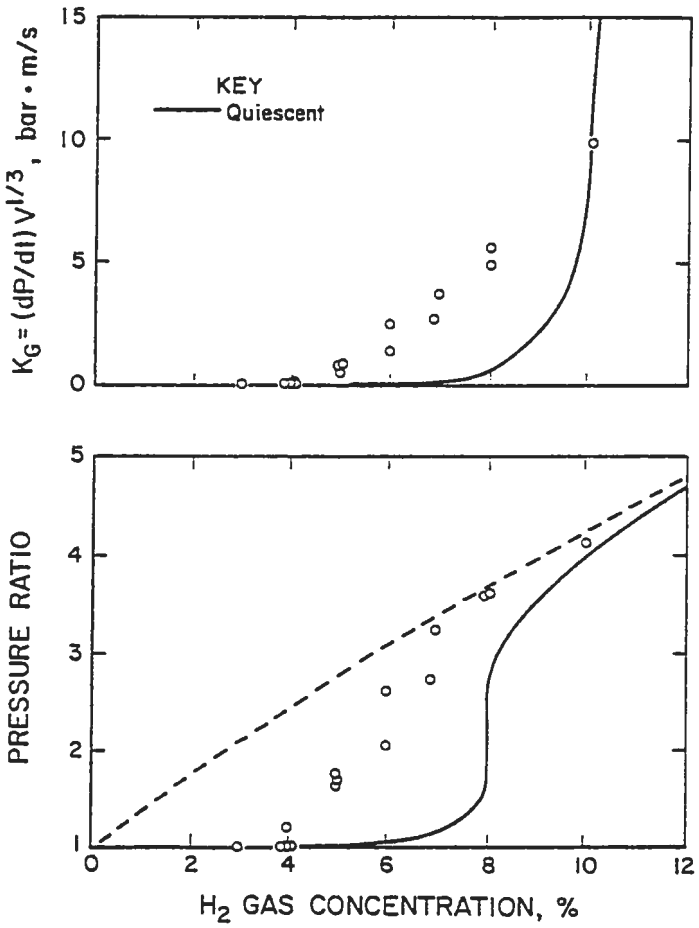

Figure 13. Flammability data (open circles) near the LFL for "turbulent" mixtures of hydrogen in air in 120-L chamber, compared to solid curve for quiescent experimental data and to dashed curve for calculated adiabatic values.

the quiescent case (solid curve in fig. 13), the observed pressure rise at 6% H_2 is only a trivial fraction of the calculated, adiabatic value. The effect of turbulence is to increase the flame speed, which greatly reduces the limitations of buoyancy. This causes the propagation to be more isotropic, and the consumed flammable volume to be larger. Accordingly, the pressure rise for turbulent propagation in the transition zone is larger, as is observed in figure 13. An equivalent physical argument is to note that turbulence generates eddies of burned gas which are shed ahead of the flame-front in all directions. Eddies that are shed downward or in the horizontal direction or even upward can go well beyond the restricting cone angle, and they serve as multiple ignition sources that are absent for the quiescent, laminar case under buoyancy control. Based on the previous 7% pressure rise criterion, the turbulent LFL $\simeq$ 4%, comparable to the LFL for quiescent H_2-air in flammability tubes using a visual criterion (*3*). These data on the effects of turbulence on H_2 flammability are consistent with some earlier PRL data from an 8-L chamber (*23*) and those of other researchers (*24,25*).

Hydrogen-air, quiescent, 5000-J ignitor

The data in figure 14 are for H_2-air mixtures that were tested with a strong 5000-J pyrotechnic source in the 120-L chamber. To calculate the pressure ratios for the 5000-J ignitor tests in the 120-L chamber, the pressure rise of the ignitor by itself was subtracted from the maximum explosion pressure (eqn. 3). However, as discussed for the CH_4 data, this did not correct entirely for the effects of the large ignitor flame. During a test, any H_2 gas that was within the ignitor flame would burn, regardless of whether flame would propagate beyond the ignitor. Therefore, even at 3 to 4% H_2, there was a measurable pressure ratio of 1.1 to 1.2 in figure 14. These low pressure ratios are not considered to be

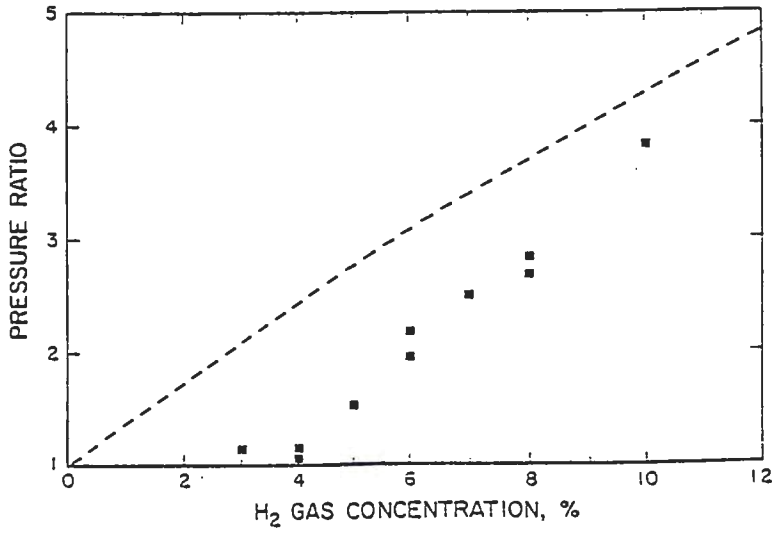

Figure 14. Flammability data for quiescent mixtures of hydrogen in air in 120-L chamber, using 5000-J pyrotechnic ignitors.

evidence of flame propagation when the 5000-J ignitors are used. Based on the previous criterion of PR $\geq$ 1.5 for upward flame propagation with the Sobbe ignitors, LFL $\simeq$ 5$\pm$½% under these test conditions. The 5000-J ignitor data further reinforce the viewpoints on turbulence from the preceding paragraphs because this pyrotechnic source induces turbulence in the test mixture. It also produces a large flame directed across the chamber toward the opposite wall rather than being a point source like the spark. Both of these effects negate the geometric limitations of buoyancy-controlled propagation from a point source. As a result, the data for the 5000-J pyrotechnic ignitor show a similar pressure increase versus H_2 concentration as was observed for the turbulent case (fig. 13). The measured explosion pressure for the 5000-J ignitor at 6% H_2 is about one-half the calculated adiabatic value.

In previous flammability experiments with the 5000-J ignitor in a 20-L chamber (*6*) and in the data in figure 8 for CH_4 in the 120-L chamber, there was evidence that this strong ignitor could "overdrive" the system. The measured pressure ratios for H_2 mixtures at 4% and below shown in figure 14 are quite low, however, and suggest no significant overdriving for the 5000-J ignitor with H_2-air in the 120-L chamber. There is less "overdriving" by the 5000-J ignitors for the H_2 than for CH_4 (fig. 8) since there is much less combustion energy available at 4% H_2-air than at 5% CH_4-air, as shown by the relative adiabatic pressures.

Deuterium-air, quiescent, spark

Deuterium (D_2), the heavier isotope of hydrogen, was tested to evaluate the effects of diffusivity on hydrogen flammability. Chemically, hydrogen and deuterium are virtually identical, but the lighter isotope's diffusivity is 1.86 cm^2/s, compared to 1.32 cm^2/s for deuterium (*5*). The 120-L data obtained for initially quiescent D_2-air mixtures with spark ignition are shown in figure 15. The measured pressure ratios are compared with the experimental data for H_2-air mixtures (chain-dashed curve) and with the calculated, adiabatic equilibrium explosion pressures for constant volume D_2 combustion (dashed curve). In this case, the downward flame propagation limit has shifted from about 8% H_2 to about 9½% D_2. Koroll and Kumar (*26*) report higher downward flame limits in a flammability tube: 9.0% for H_2 and 10.2% for D_2. The data in figure 15 show that selective diffusion has less of an effect for the deuterium than for the hydrogen, as expected due to its lower diffusivity. Based on the 7% pressure rise criterion, the LFL $\simeq$ 7½$\pm$½% for upward flame propagation of D_2-air in the 120-L chamber, compared to the LFL $\simeq$ 6½$\pm$½% for H_2-air. Koroll and Kumar (*26*) report upward flame limits in a flammability tube of 4.0% for H_2 and 5.6% for D_2.

Deuterium-air was also tested as "turbulent" mixtures by allowing the fan to run during ignition. Based on the previous 7% pressure rise criterion, the turbulent LFL $\simeq$ 5½% for D_2-air. This value is comparable to the LFL reported for D_2-air in flammability tubes, using a visual criterion (*26*).

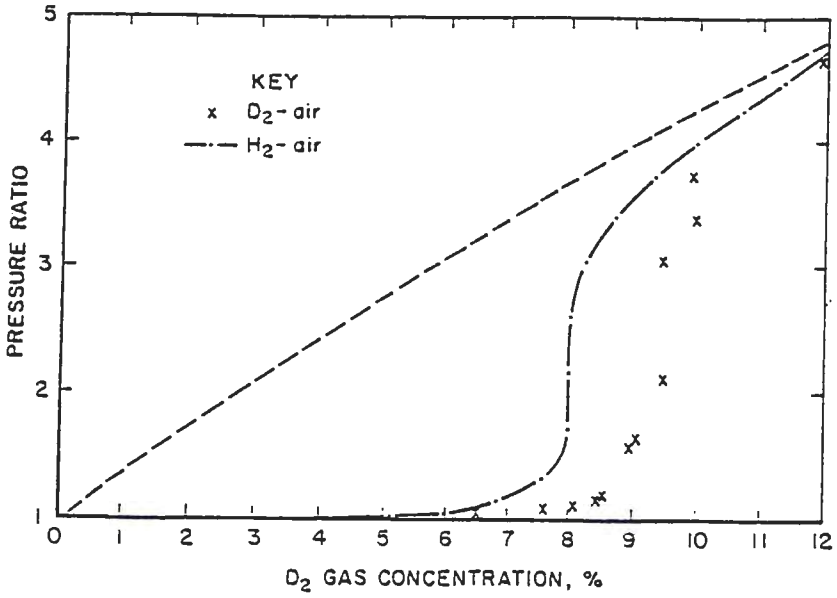

Figure 15. Flammability data for quiescent mixtures of deuterium (D_2) in air in 120-L chamber, compared to dot-dashed curve for H_2-air and to dashed curve for calculated adiabatic values.

Discussion and Conclusions

A summary of the flammability limit data for methane, propane, hydrogen, and deuterium gases in air is listed in table I. All of the data were for initially quiescent mixtures, using spark ignition. The LFL data using a visual criterion for flame propagation were from earlier data in flammability tubes (*3,22,26*) and in the 25.5-m^3 spherical chamber (*15*). The LFL values using a pressure rise criterion of either 3% (0.5 psi) or 7% (1 psi) were from the present data in the 20-L and 120-L chambers and from the earlier 25.5-m^3 data (*12,15*). The UFL data were from earlier flammability tube data (*3*) using a visual criterion and from the present 20-L and 120-L data using a pressure rise criterion. The methane LFL values show very close agreement, regardless of whether a visual criterion or a 3% or 7% pressure rise criterion was used. In all cases, the LFL for methane in air was close to 5.0% CH_4. The UFL for methane was somewhat higher in the 20-L and 120-L closed chambers than in the flammability tube.

The propane LFL value from the 120-L chamber using either the 3% or 7% pressure rise criterion was comparable to the LFL from the flammability tube. The UFL for propane was slightly higher in the 120-L closed chamber than in the flammability tube.

The hydrogen flammability limit values show a large dependence on the propagation criterion chosen. The limit for visual observation of flame is about 4% H_2, but the measured pressure rise at this concentration is close to zero. Significantly higher H_2 concentrations are needed to reach a pressure rise of 7% (0.07 bar or 1 psi). The LFL for deuterium using the 7% pressure rise criterion was also higher than that measured in the flammability tube using

Table I. - Flammable Limits of Gases (in volume %) for upward flame propagation in quiescent mixtures, with spark ignition

	Methane, CH_4	Propane, C_3H_8	Hydrogen, H_2	Deuterium, D_2
Lower Flammable Limit (LFL), *using a visual criterion*				
Flammability tube (Refs. *3,25,26*)	5.0	2.1	4.0	5.6
25.5-m^3 sphere (Ref. *15*)	4.9	–	<5	–
Lower Flammable Limit (LFL), *using pressure rise criterion of 3% (0.03 bar or ½ psi)*				
20-L chamber	4.9±0.1	–	5±½	–
120-L sphere	5.0±0.1	2.05±0.05	5±½	–
Lower Flammable Limit (LFL), *using pressure rise criterion of 7% (0.07 bar or 1 psi)*				
20-L chamber	5.0±0.1	–	6±½	–
120-L sphere	5.0±0.1	2.05±0.05	6½±½	7½±½
25.5-m^3 sphere (Refs. *12,15*)	5.1±0.1	–	7½±½	–
Upper Flammable Limit (UFL), *using a visual criterion*				
Flammability tube (Ref. *3*)	15.0	9.5	75	–
Upper Flammable Limit (UFL), *using pressure rise criterion of 7% (0.07 bar or 1 psi)*				
20-L chamber	15.9±0.1	–	–	–
120-L sphere	15.7±0.2	9.8±0.2	–	–

a visual criterion. The data in the table also show that the hydrogen LFL based on this pressure criterion is higher in larger chambers. The LFL values were 6%, 6½%, and 7½% for H_2-air in 20-L, 120-L, and 25.5-m^3 chambers, respectively. An explanation is that a fireball propagating only in the upward direction will constitute an increasingly smaller fraction of the chamber volume for larger chambers. Therefore, the corresponding pressure rise at a given H_2 concentration will be less in larger chambers. It follows that the flame propagation criteria chosen and consequently the resulting flammability limits are somewhat arbitrary. For practical applications of the flammability limit data, one should compare the measured pressures under various test conditions with the rated pressures of the vessels to be protected.

A summary of the maximum explosion pressures and normalized rates of pressure rise (K_G) is listed in table II. The maximum measured explosion pressures for methane-air and propane-air in the 120-L chamber were about 95% of the calculated values for adiabatic combustion. The P_{max} value for CH_4-air in the 20-L chamber was slightly lower. The measured explosion pressures in the 25.5-m^3 chamber (*13,14*) were reported at stoichiometric concentrations, and may be slightly lower than would be found at concentrations slightly

Table II. - Maximum Pressures and Rates of Pressure Rise for Gases

	Methane, CH_4	Propane, C_3H_8	Hydrogen, H_2
Maximum Pressures (P_{max}) *in bar,g*			
calculated, adiabatic	7.9	8.6	7.1
20-L chamber	7.3±0.1	–	–
120-L sphere	7.5±0.1	8.2±0.2	7.1±0.1
25-m^3 sphere (Ref. *13,14*)	6.6±0.1*	7.8±0.5*	–
Maximum Rates of Pressure Rise (K_G) *in bar·m/s*			
20-L chamber	66±2	–	–
120-L sphere	92±3	150±20	1260±70
25-m^3 sphere (Ref. *13,14*)	110±8*	~400±100*	–

* data at stoichiometric only

above stoichiometric. With this correction, the P_{max} value for C_3H_8-air in the 25.5-m^3 chamber would be close to the value in the 120-L chamber, but P_{max} for CH_4-air in the 25.5-m^3 chamber would still be lower than the value in the 120-L chamber. For H_2-air, which burns much faster than CH_4 or C_3H_8, the P_{max} value in the 120-L chamber is the same as the calculated, adiabatic value. The K_G values for CH_4-air show an increase with vessel size, perhaps due to greater flame induced turbulence in the larger chambers.

Acknowledgments

The authors wish to acknowledge the financial support of the U.S. Department of Energy and its site contractors Westinghouse Hanford Company and Westinghouse Savannah River Company for parts of this research, particularly for the sections on hydrogen flammability.

References

1. Coward, H. F., and G. W. Jones. Limits of Flammability of Gases and Vapors. Bureau of Mines Bulletin 503, 1952, 155 pp.

2. Zabetakis, M. G. Flammability Characteristics of Combustible Gases and Vapors. Bureau of Mines Bulletin 627, 1965, 121 pp.

3. Kuchta, J. M. Investigation of Fire and Explosion Accidents in the Chemical, Mining, and Fuel-Related Industries - A Manual. Bureau of Mines Bulletin 680, 1985, 84 pp.

4. Hertzberg, M. The Theory of Flammability Limits: Radiative Losses and Selective Diffusional Demixing. Bureau of Mines RI 8607, 1982, 38 pp.

5. Hertzberg, M. Selective Diffusional Demixing: Occurrence and Size of Cellular Flames. Prog. Energy Combust. Sci., v. 15, 1989, pp. 203-239.

6. Hertzberg, M., K. L. Cashdollar, and I. A. Zlochower. Flammability Limit Measurements for Dusts and Gases. Paper in Twenty-First Symposium (International) on Combustion, The Combustion Institute, Pittsburgh, PA., 1988, pp. 303-313.

7. Cashdollar, K. L., M. Hertzberg, I. A. Zlochower, C. E. Lucci, G. M. Green, and R. A. Thomas. Laboratory Flammability Studies of Mixtures of Hydrogen, Nitrous Oxide, and Air. Final Report to Westinghouse Hanford Company, Richland, WA, June 1992, (published as WHC-SD-WM-ES-219, Revision 0, September 1992, 71 pp.)

8. Zlochower, I. A., K. L. Cashdollar, and G. M. Green. Measurement of the Lower Flammability Limits of Mixtures of Volatile Organic Compounds plus Hydrogen in Air. Final Report to Lockheed Martin Idaho Technologies Company, Idaho Falls, ID, September 1997, (published as Appendix B of INEEL 97/*xxxx*, Flammability Assessment Methodology Program Phase I: Final Report, by C. A. Loehr, S. M. Djordjevic, K. J. Liekhus, M. J. Connolly, Idaho National Engineering and Environmental Laboratory, Lockheed Martin Idaho Technologies Company, Idaho Falls, ID, September 1997)

9. Hertzberg, M., R. S. Conti, and K. L. Cashdollar. Electrical Ignition Energies and Thermal Autoignition Temperatures for Evaluating Explosion Hazards of Dusts. Bureau of Mines RI 8988, 1985, 41 pp.

10. Lüttgens, G., and M. Glor. *Understanding and Controlling Static Electricity*. Expert Verlag, Ehningen bei Böblingen, Germany 1989, p. 159.

11. Eckhoff, R. K. *Dust Explosions in the Process Industries*. Butterworth Heinemann, Oxford, UK, 1991, p. 17.

12. Furno, A., E. B. Cook, J. M. Kuchta, and D. S. Burgess. Some Observations on Near-Limit Flames. Paper in the Thirteenth Symposium (International) on Combustion, The Combustion Institute, Pittsburgh, PA, 1970, pp. 593-599.

13. Nagy, J., E. C. Seiler, J. W. Conn, and H. C. Verakis. Explosion Development in Closed Vessels. Bureau of Mines RI 7507, 1971, 50 pp.

14. Sapko, M. J., A. L. Furno, and J. M. Kuchta. Flame and Pressure Development of Large-Scale CH_4-Air-N_2 Explosions. BuMines RI 8176, 1976, 32 pp.

15. Burgess, D. S., A. L. Furno, J. M. Kuchta, and K. E. Mura. Flammability of Mixed Gases. BuMines RI 8709, 1982, 20 pp.

16. Gordon, S., and B. J. McBride. Computer Program for Calculation of Complex Chemical Equilibrium Compositions, Rocket Performance, Incident and Reflected Shocks, and Chapman-Jouguet Detonations. NASA SP-273, 1976, 241 pp.

17. Chase, M. W., Jr., C. A. Davies, J. R. Downey, Jr., D. J. Frurip, R. A. McDonald, and A. N. Syverud. JANAF Thermochemical Tables, Third Edition. (Thermal Group, Dow Chemical U.S.A., Midland, MI), Journal of Physical and Chemical Reference Data, v. 14, supplement 1, 1985.

18. Hertzberg, M., K. Cashdollar, C. Litton, and D. Burgess. The Diffusion Flame in Fire Convection. Buoyancy - Induced Flames Oscillations, Radiative Balance, and Large-Scale Limiting Rates. BuMines RI 8263, 1978, 33 pp.

19. Hertzberg, M. The Theory of Flammability Limits: Natural Convection. BuMines RI 8127, 1976, 15 pp.

20. American Society for Testing and Materials. Standard Practice for Determining Limits of Flammability of Chemicals at Elevated Temperature and Pressure. E 918-83 in 1991 Annual Book of ASTM Standards: Volume 14.02, General Test Methods, Philadelphia, PA, 1991, pp. 637-641.

21. Goldmann, F. Über Difffusionserscheinungen an der unteren Explosionsgrenze von Wasserstoffknallgas (Diffusion Phenomena at the Lower Explosion Limit of Hydrogen-Oxygen Mixtures). Z. Phys. Chem., v. B5, 1929, pp. 307-315.

22. Kumar, R. K. Flammability Limits of Hydrogen-Oxygen-Diluent Mixtures. J. Fire Sci., v. 3, 1985, pp. 245-262.

23. Hertzberg, M., and K. L. Cashdollar. Flammability Behavior and Pressure Development of Hydrogen Mixtures in Containment Volumes. Paper in Thermal-Hydraulics of Nuclear Reactors, American Nuclear Society, LaGrange Park, IL, v. I, 1983, pp. 29-37.

24. Cummings, J. C., W. B. Benedick, and P. G. Prassinos. Hydrogen Combustion Results From the Sandia Intermediate-Scale (VGES) Tank and the Sandia Critical-Tube-Diameter Test Facility. Paper in Thermal-Hydraulics of Nuclear Reactors, American Nuclear Society, LaGrange Park, IL, v. II, 1983, pp. 1212-1218.

25. Kumar, R. K., H. Tamm, W. C. Harrison, G. Skeet, and J. Swiddle. Combustion of Hydrogen at High Concentrations Including the Effect of Obstacles. Paper in Thermal-Hydraulics of Nuclear Reactors, American Nuclear Society, LaGrange Park, IL, v. II, 1983, pp. 1203-1211.

26. Koroll, G. W., and R. K. Kumar. Isotope Effects on the Combustion Properties of Deuterium and Hydrogen. Combust. Flame, v. 84, 1991, pp. 154-159.